Supplementary Materials for

High precision, high throughput generation of single cells containing droplets

Jiande Zhou[1]*, Amaury Wei[1], Arnaud Bertsch[1], Philippe Renaud[1]*

*Corresponding author. Email: jiande.zhou@epfl.ch ; philippe.renaud@epfl.ch

This PDF file includes:

Supplementary Text
Figures. S1 to S5
Movie S1

Other Supplementary Materials for this manuscript include the following:

Movie S1

Supplementary text

Section 1: Chip Design and T junction geometrical rule

The overall chip design is shown in Fig. S1a, where blue dotted box highlights each functional unit. Four inlets are included (red). Inlets 1 & 2 introduce cell medium and oil (continuous phase) for droplet generation, inlet 3 (oil) is for droplet spacing and inlet 4 (oil) is for introducing pinching flow for PFF operation. The oil inlets have a filter structure at the entrance to avoid debris into the system. There are five main outlets, the bottom one is for single cell droplet collection. It is critical to add the resistive meanders at the end of each outlet, to ensure the sorting stability. A short bypass outlet (yellow) is created upstream to the T junction and spacing channel which evacuates all the waste and debris during priming of the system. It is blocked when the operation starts. We found that this strategy avoids most of the clogging issue despite of the critical dimension in T junction (i.e., 11 μm). The structure within the grey dotted box is zoomed-in in Fig.S1b and c. An expansion angle A is deployed at the end of the T junction outlet to limit the duration of cell squeezing. This expansion is not necessary for the cell triggered splitting (CTS) function as we also observed the CTS on T junctions without this expansion i.e., with a straight channel until the end.

Eq.1 is a geometrical design rule for designing a T junction that is capable of the capillary instability leading to lateral breakup (LB) and thus CTS, which is a prerequisite for the method we show in this study.[34] For any (deformable) object to be encapsulated, the design of geometry includes the following steps: first, w_o is chosen to be slightly smaller than the target object size. For relatively more rigid objects, the dimension difference between the object size and the w_o can be smaller. Then, the width ratio ($\frac{w_i}{w_o}$) and aspect ratio ($\frac{w_i}{h}$) can be chosen according to Eq.1 and according to the throughput requirement. A rare cell sample normally has small sample volume and might require a lower flow rate, while large sample might prefer a higher throughput. In the main text, we show that throughput can be adjusted by merely changing the operational flow condition along the transition flow conditions. In addition to that we also found that geometry can alter the position of the transition boundary[34], thus determining the bounded effective throughput range within which the flow condition can make an adjustment. Indeed, we found that the critical flowrates at which the breakup regimes start to change is influenced slightly by the expansion angle A, constriction channel length N, but significantly by the width ratio ($\frac{w_i}{w_o}$) and aspect ratio ($\frac{w_i}{h}$). A general rule is that increasing one or both of the ratio(s) would push the transition to happen at higher flowrates, and thus operating with higher throughput. This is an important factor when considering the design of the geometry for different applications. In this study, we used a T junction $A = 4°$, $N = 50\ \mu m$, $w_i = 30\mu m$, $w_o = 10\mu m$ and $h = 52\ \mu m$ for encapsulation experiment with HT-29 cells. We used a T junction with $A = 4°$, $N = 250\ \mu m$, $w_i = 120\mu m$, $w_o = 55\mu m$ and $h = 180\ \mu m$ for encapsulation experiment with the 10x genomics bead.

$$\beta = 2\frac{w_i/w_o}{1+\frac{w_i}{h}+\sqrt{\left[\left(1-\frac{w_i}{h}\right)^2+\pi\frac{w_i}{h}\right]}} > 1 \quad (1)$$

Now we explain the simple procedures to determine the operational condition. First, determine a suitable flow rate for the cell medium (inlet 1) according to the sample volume; second,

gradually increase the oil flow rates of the inlet 2 and 3 until the transition from LB to CB occurs, this flow condition is the operational condition. Many operational conditions are possible and thus it is easy to find one. No need to determine a full regime map prior to the use of the chip. Once the operational condition is empirically pre-determined, it can be directly applied during the formal experiment.

Section 2: Single cell triggering process

To illustrate the process of CTS, we used a high-speed camera to capture the different breakup procedures experienced by the two types of mother droplets - empty droplets and single cell containing droplets- at the same flow condition and on the same geometry (Fig.S2). Take the moment when the droplet rear interface has fully entered the outlet channel as time zero, at T = 20 ms, an empty droplet finishes breaking centrally; for a cell loaded droplet however, no sign of central breakup occurs at T = 20 ms, due to the retardation of the cell at the junction; until T = 27 ms the lateral breakup has happened, with a droplet interface splitting in one arm of the T junction, generating the satellite droplet around the junction area, where the cell resides, thus encapsulating the cell automatically.

Section 3: Cell triggering efficiency @ 241 Hz

We summarize the single cell triggering efficiency at throughput of 241Hz as shown in Fig.S3. While the triggering efficiency for cells smaller than or similar to the outlet channel width w_o ($w_o = 11\mu m$) is not as sufficient as @ 47 Hz, the triggering efficiency for cells that are equal to or larger than 12 μm remains > 95%. This indicates a highly selective triggering with a cutoff triggering threshold at 12 μm, i.e., at a cell size slightly larger than w_o. Such knowledge can be used to design a chip for either full population encapsulation, i.e., redesigning of a w_o that is smaller than the full-size spectrum of the cell population, or a size-selective encapsulation, i.e., redesigning of a w_o that is only smaller than the size of target cells but similar to or larger than the rest of the cell population.

At throughput of 3100 Hz, due to the difficulties in assessing the cell size limited by the image quality, the triggering efficiency at different cell size range cannot be obtained. However, the overall triggering efficiency is close to Fig.S3. We could assume the same triggering threshold is playing a role.

Section 4: Droplet size distribution

The droplet size distribution for both experiments at 47Hz and at 241 Hz are shown in in Fig.S4.

Section 5: Self correction

Here we show a typical encapsulation process for a mother droplet containing two cells. When the two cells are separated from each other within the droplet, the front cell is pushed through the junction while only the second cell is encapsulated in the satellite droplet. As a result, the doublets are self-corrected during the process of CTS.

Note, if the two cells are adherent to each other, the junction cannot separate them, and the two cells are encapsulated together (as a single object) into the same satellite droplet.

Supplementary figures

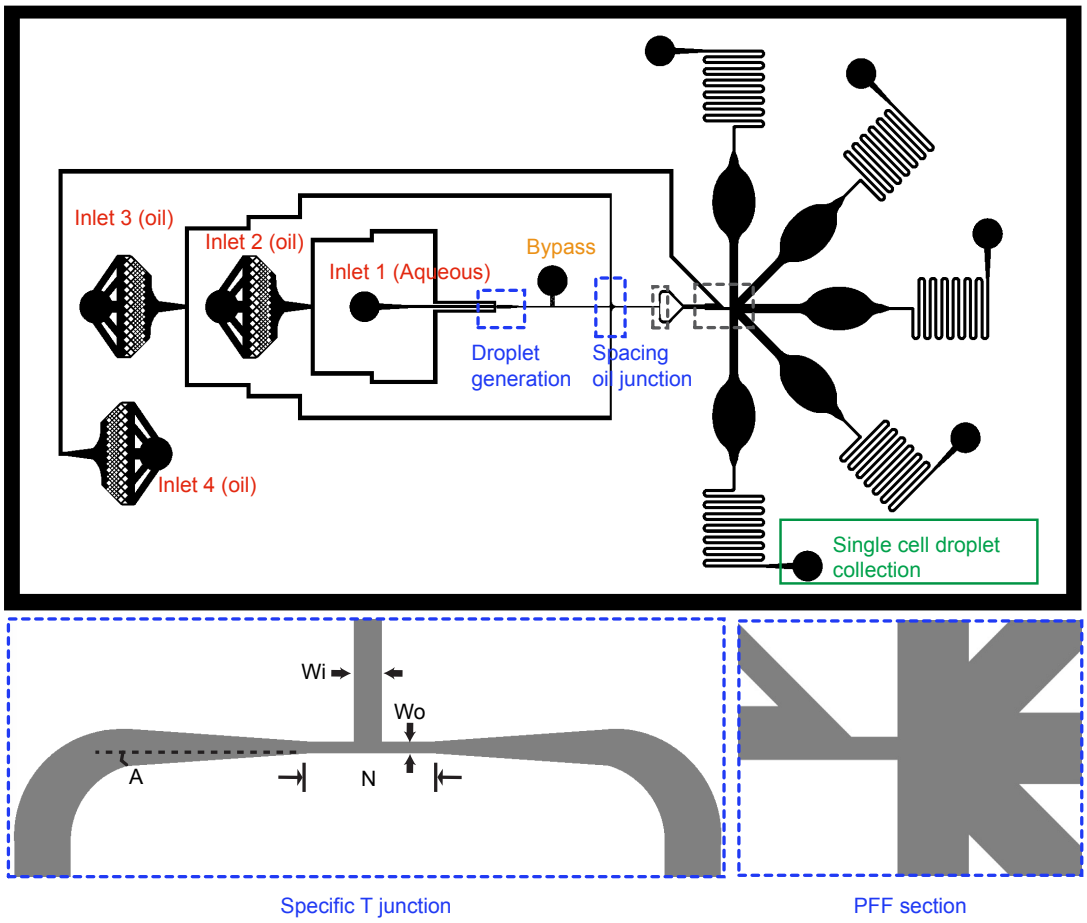

Fig. S1.

The chip design presentation and definition of parameters. The inlets are shown in red; the blue dotted boxes show the different microfluidics units, including droplet generation, droplet spacing, specific T junction (bottom panel, zoomed-in of the grey dotted box) and PFF (bottom panel, zoomed-in of the grey dotted box.

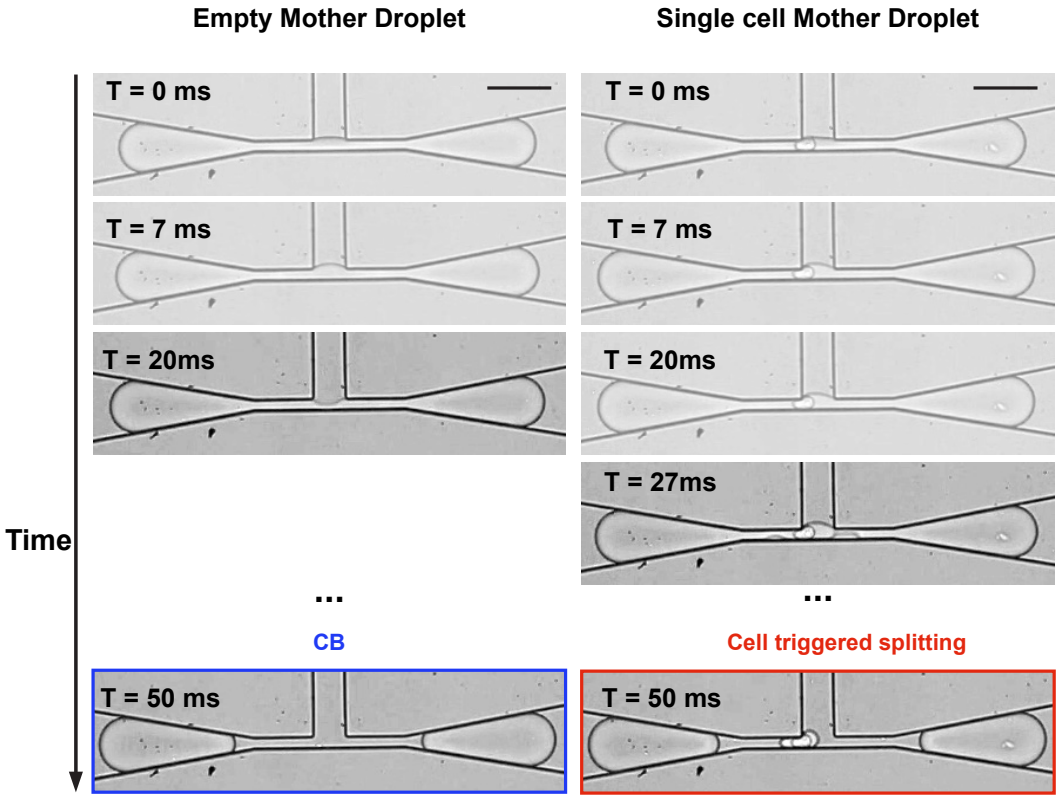

Fig. S2.

The Cell triggered Differential Splitting. Time sequences of two breakup events. For single cell containing mother droplet, the central breakup does not happen at T = 20 ms as for the empty droplet; at T = 27 ms, the lateral breakup process is completed. The bottom panels show the final breakup results. Scale bar = 60 μm.

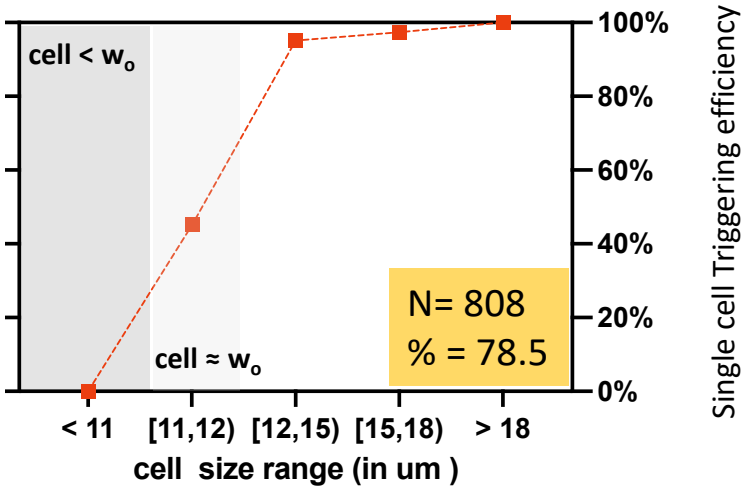

Fig. S3.

Single cell triggering efficiency at different cell size categories obtained @ 241Hz. The cell size range for each cell size category is shown in the x axis; the cell triggering efficiency for each category is shown in the y axis; the yellow box indicates total cell number and the overall triggering efficiency for the total cell population.

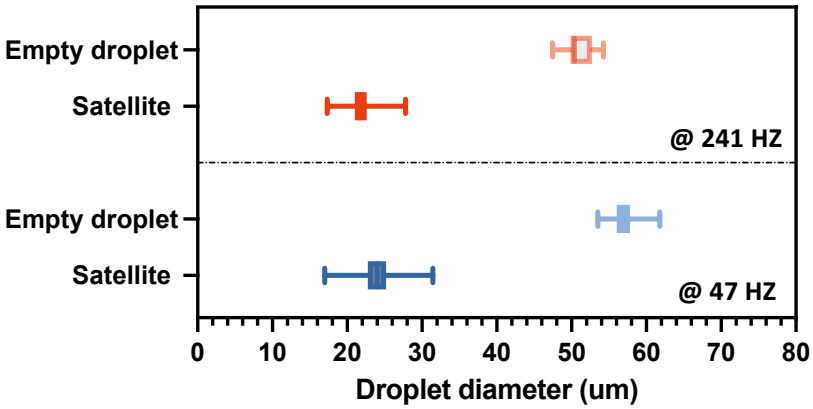

Fig. S4.

The droplet size distribution @ 241Hz and @ 47Hz. The min and max values are shown as the whiskers, the 1st and 3rd quartiles are shown in box, with median show as the darker line inside the box.

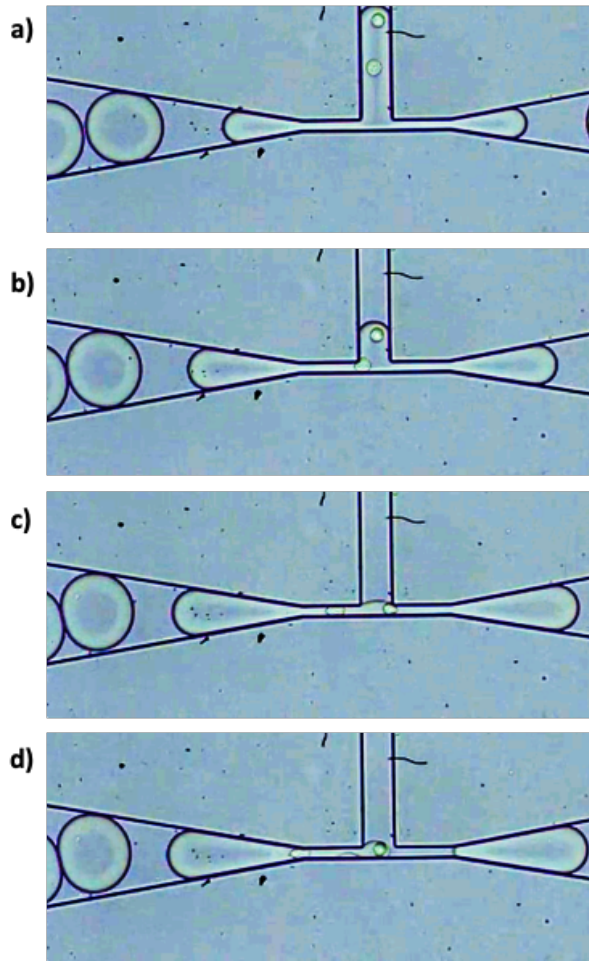

Fig S5.

The time sequence of a droplet splitting event with two cells.

Movie S1

Slow motion_Cell Triggered Splitting. mov

Example of four droplet splitting events (two empty and two with a single cell) taken by the high-speed camera under a framerate of 3,000 FPS.